ELSEVIER

Journal of Fluids and Structures 21 (2005) 103–119

JOURNAL OF FLUIDS AND STRUCTURES

www.elsevier.com/locate/jfs

Flow-excited acoustic resonance of two tandem cylinders in cross-flow

A. Mohany*, S. Ziada

Department of Mechanical Engineering, McMaster University, 1280 Main Street West, Hamilton, Ont., Canada L8S 4L7

Received 5 October 2004; accepted 28 May 2005

Abstract

The aeroacoustic response of two tandem cylinders in cross-flow is investigated experimentally. Eleven spacing ratios between the cylinders, in the range of $L/D = 1.2-4.5$, have been tested to investigate the effect of the gap between the cylinders on the excitation mechanism of acoustic resonance. During the tests, the acoustic cross-modes of the duct housing the cylinders are self-excited. Similar tests are performed on isolated cylinders. The aeroacoustic response of the tandem cylinders is found to be considerably different from that of isolated cylinders. For isolated cylinders, acoustic resonance of a given mode occurs over a single range of flow velocity and is excited by the natural vortex shedding process observed in the absence of acoustic resonance. In the case of tandem cylinders with a spacing ratio inside the proximity region, L/D is less than 3.5, the resonance occurs over two different ranges of flow velocity. One of these ranges is similar to that observed for isolated cylinders and the other occurs at much lower flow velocities. The latter resonance range seems to be triggered by the instability of the separated flow in the gap between the cylinders. Outside the proximity region, the aeroacoustic response of the two tandem cylinders is similar to that of isolated cylinder.

Keywords: Tandem cylinders; Vortex shedding; Acoustic resonance; Flow–acoustic interaction

1. Introduction

The phenomenon of vortex shedding has been a subject of research since it was observed by Leonard da Vinci, even though there is much that remains to be understood. Vortex shedding from cylinders in cross-flow generates sound which reflects back from the surrounding surfaces and creates a feedback cycle that enhances the shedding process. Understanding the feedback cycle of the flow-excited acoustic resonance will help to control and avoid the occurrence of the acoustic resonance.

Flow-excited acoustic resonance of ducts containing clusters of bluff bodies is a design concern in many engineering applications, such as tube bundles of heat exchangers and boilers (Blevins and Bressler, 1993; Oengören and Ziada, 1998), cascades of compressor blades (Parker and Pryce, 1974) and guide/turning vanes in ducts and radial diffusers (Ziada et al., 2002). When these resonances are excited, the resulting acoustic pressure may exceed the dynamic head of the mean flow. This can be sufficiently high to cause acute noise and/or vibration problems in diverse industrial equipment, such as those mentioned above.

*Corresponding author. Tel.: +1 905 525 9140; fax: +1 905 572 7944.
E-mail address: mohanyam@mcmaster.ca (A. Mohany).

0889-9746/$ - see front matter © 2005 Elsevier Ltd. All rights reserved.
doi:10.1016/j.jfluidstructs.2005.05.018

Nomenclature

c	speed of sound
C_L	coefficient of oscillating lift force acting on the cylinder
C_d	coefficient of oscillating drag force acting on the cylinder
D	cylinder diameter
f_a	frequency of the lowest acoustic resonance mode of the test section
f_v	vortex shedding frequency
H	height of the duct
k	wavenumber
L	center to center distance between cylinders
l	cylinder length
M	Mach number
P_{rms}	acoustic pressure (root mean square amplitude)
p	radiated sound pressure
P^*	normalized sound pressure
R	distance in the flow field from the cylinder axis
St	Strouhal number of vortex shedding
t	time
U	upstream flow velocity
U_r	reduced velocity
$\boldsymbol{u}$	acoustic particle velocity
$\boldsymbol{v}$	local flow velocity

Greek letters

β	phase shift
θ, ϕ	angles of the far field observer with respect to the cylinder axis
λ	wavelength of the acoustic wave
Π	the instantaneous acoustic power
ρ	air density
ω	vorticity

The resonance occurs when the frequency of vortex shedding from the bluff body, f_v, approaches that of an acoustic mode, f_a. As the acoustic mode is excited by the dipole-like source of vortex shedding (Curle, 1955), the resulting sound field of the resonant acoustic mode enhances the process of vortex shedding, and essentially a lock-in mechanism, or synchronization is generated, by which both the shedding process and the resonant mode enhance each other, as shown in Fig. 1. Parker and Stoneman (1989) and Welsh et al. (1990) have published excellent reviews of flow-excited acoustic resonances. A crucial event in the mechanism of acoustic resonance is the ability of sound to modulate, and essentially "lock-in", the process of vortex shedding. While this phenomenon is relatively well understood for the case of *isolated* cylinders (Blevins, 1985), there are many unresolved issues for the more complex case of multiple cylinders in close proximity, such as tube bundles.

Hall et al. (2003) studied the effect of sound on vortex shedding from two tandem cylinders. They reported that the lock-in region was much wider than in the case of a single cylinder. In other words, tandem cylinders in cross-flow are much more liable to acoustic resonance excitation than isolated cylinders. Since the sound field in the experiments of Hall et al. (2003) was not self-generated, but rather, externally imposed, it is not possible to predict the range of flow velocity over which acoustic resonance will be self-excited. Fitzpatrick (2003) investigated sound generation by vortex shedding from two tandem cylinders in cross-flow. However, the acoustic natural frequency of the wind tunnel was far removed from the vortex shedding frequency and therefore self-excited acoustic resonance and the associated flow/sound interaction mechanism were not investigated. For the case of self-excited acoustic resonance, Blevins and Bressler (1993) have performed experiments on the acoustic resonance in heat exchanger tube bundles. The first phase of their experiments focused on the aeroacoustic response of a single cylinder in cross-flow under resonance conditions, and the second phase investigated the aeroacoustic response of different tube array configurations. The main objective of these experiments was to develop a model that can be used to predict the resonant sound pressure level for a single and multiple cylinders in cross-flows.

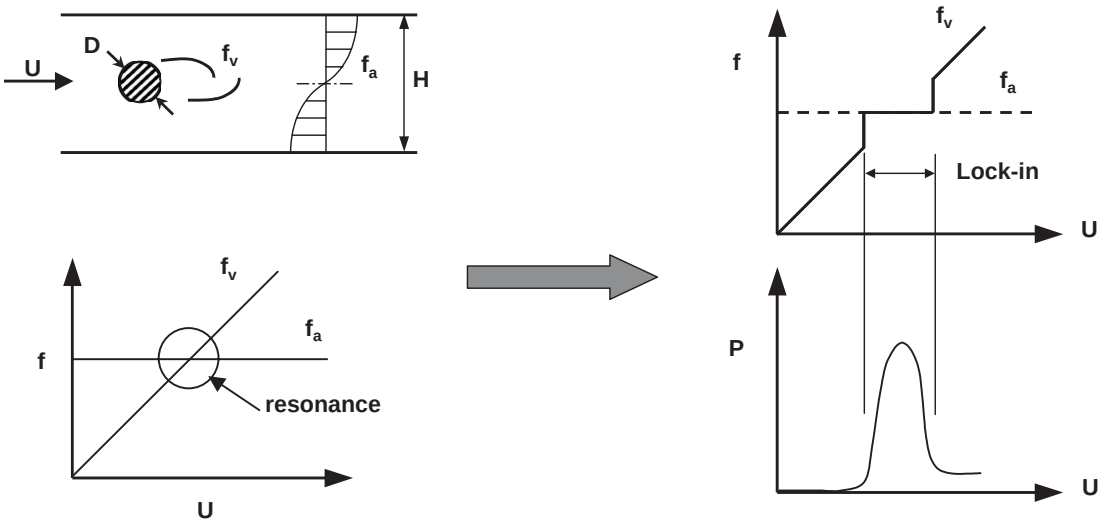

Fig. 1. Schematic presentation for the lock-in phenomenon, and the main features of flow-excited acoustic resonance.

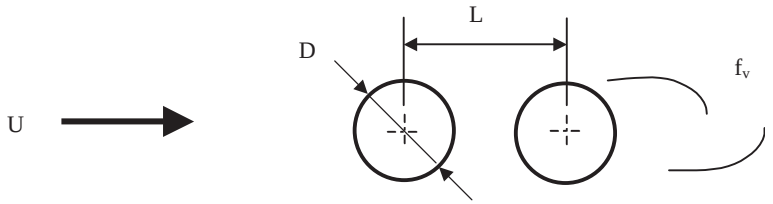

Fig. 2. The tandem cylinders arrangement.

In the present study, an experimental setup is designed, which is conducive to self-generation of acoustic resonance of a duct housing two tandem cylinders in cross-flow. The objective is to examine the effect of varying the distance between the two cylinders on the acoustic resonance mechanism. Tests are performed on both isolated cylinders, with four different diameters, and two tandem cylinders with eleven spacing ratios between the cylinders in the range of $L/D = 1.2-4.5$, where L is center-to-center distance between the cylinders and D is the cylinder diameter, as shown in Fig. 2. Special attention is given to the proximity interference region in which the spacing ratio is less than 3.5 (Zdravkovich, 1977). However, two spacing ratios in the wake interference region, $L/D > 3.5$, are also tested to compare their aeroacoustic response with the unique response that was observed for the tandem cylinders inside the proximity interference region. In the absence of sound waves, this proximity-interference range is characterized by a quasi-steady reattachment of the shear layers separated from the upstream cylinder onto the rear cylinder, as discussed by Igarashi (1981) and Zdravkovich (1985). The interaction of these shear layers with sound waves is expected to affect the mechanism of acoustic resonance.

2. Experimental set-up

The experiments were performed in an open-loop wind tunnel. The test-section was made of 25.4 mm thick clear acrylic walls, to facilitate a flow-visualization study in the future, and had a cross-section of 76.2 mm in width by 254 mm in height. These dimensions were carefully selected to insure coincidence between the first acoustic resonance frequency and the frequency of vortex shedding from single and tandem cylinders. A parabolic contraction was used at the inlet to produce a uniform velocity profile with as small as possible boundary layer thickness. A flat-walled diffuser

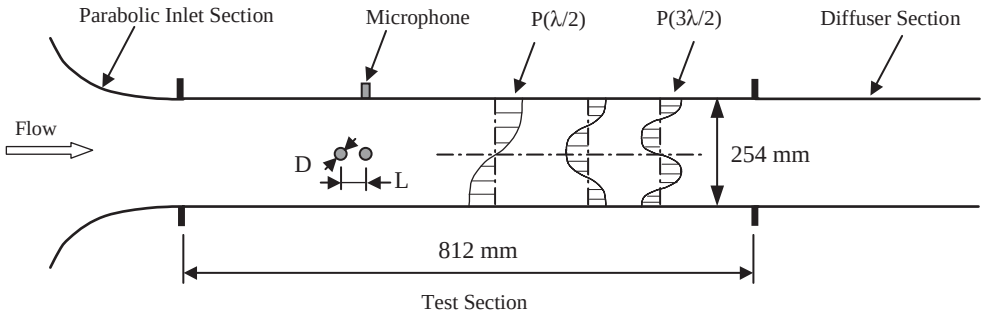

Fig. 3. Schematic drawing for the test section $P(\lambda/2)$ and $P(3\lambda/2)$ stand for the acoustic pressure distribution of the first and third cross-modes of the duct, respectively.

that expands in one direction only, with an included angle of 14°, was used downstream of the test section to increase the pressure recovery and thereby increase the maximum flow velocity during the tests. The diffuser outlet was connected to the inlet of a centrifugal blower by means of a flexible duct. This arrangement helped in reducing vibration transmission from the blower to the test-section. The blower was equipped with a 50 HP motor and a variable speed controller. With this arrangement, it was possible to achieve a maximum flow velocity of 120 m/s in the test-section.

Several cylinders with different diameters were used. The largest diameter produced a maximum wind tunnel blockage ratio less than 10%. The cylinders were made of aluminum and were machined to produce a qualitatively similar surface roughness for all cylinders. Each cylinder had two side-taps and was rigidly mounted on the test-section sidewall to eliminate the effect of cylinder vibration on the flow–sound interaction mechanism. Two windows attached to the sidewalls were used to provide flexibility in setting up different cylinder diameters, different arrangements and different spacing ratios. A general layout of the test-section is shown in Fig. 3.

During the tests, vortex shedding from the cylinder(s) excited the lowest cross-mode of the test-section, $P(\lambda/2)$, and in some cases, the third mode, $P(3\lambda/2)$, was also excited at relatively high flow velocities. The acoustic pressure distributions of these modes are illustrated in Fig. 3. They consist of standing sound waves between the top and bottom walls of the test-section. The frequency of the first, and lowest, mode can be approximated by $f = c/2H \approx 688$ Hz.

The flow velocity inside the test-section was calibrated by means of a pitot tube and a pressure transducer. Several preliminary measurements of the flow velocity at different transverse (and streamwise) positions showed that the velocity profile was uniform and within $\pm 2\%$ of the mean velocity. The fluctuating pressure on the top wall of the duct was measured by means of a $\frac{1}{4}$'' condenser microphone, which was flush-mounted in the test-section wall at the location of the maximum acoustic pressure; see Fig. 3. This location was found by measuring the acoustic pressure on the top wall at different streamwise positions for both the first and the third acoustic modes. As shown in Fig. 4, the maximum acoustic pressure for both modes occurs at the same streamwise location. All results presented here were collected by the microphone positioned at this maximum acoustic pressure location.

The experiments were performed as follows. For each spacing ratio in the tandem cylinder tests or each diameter in the single cylinder tests, the blower speed was increased by a small increment corresponding to an increase in the flow velocity inside the test-section by about 5 m/s, until the resonance occurred. Near and inside the resonance range, this increment was reduced, corresponding to an increase in the flow velocity by about 2 m/s. A Hewlett-Packard analyser was used for spectral analysis. Each spectrum was obtained by averaging 100 samples. Data was collected at a sampling rate of 4100 Hz.

3. Acoustic resonance of single cylinders

For the single cylinder case, four cylinder diameters were investigated in this study: $D = 12.7$, 15.9, 19 and 25.4 mm. The Reynolds number of these tests varied between 10^4 and 3×10^5. Fig. 5(a) shows a typical pressure spectrum for a 19 mm single cylinder in cross-flow, and Fig. 5(b) shows a waterfall plot of pressure spectra for the same cylinder. At off-resonance conditions, two frequency components can be observed in Fig. 5(a): the lower component is the vortex shedding frequency, while the higher component near 688 Hz is the first acoustic mode of the duct housing the cylinder. As the flow velocity is increased, the frequency of the vortex shedding component and its amplitude are increased until

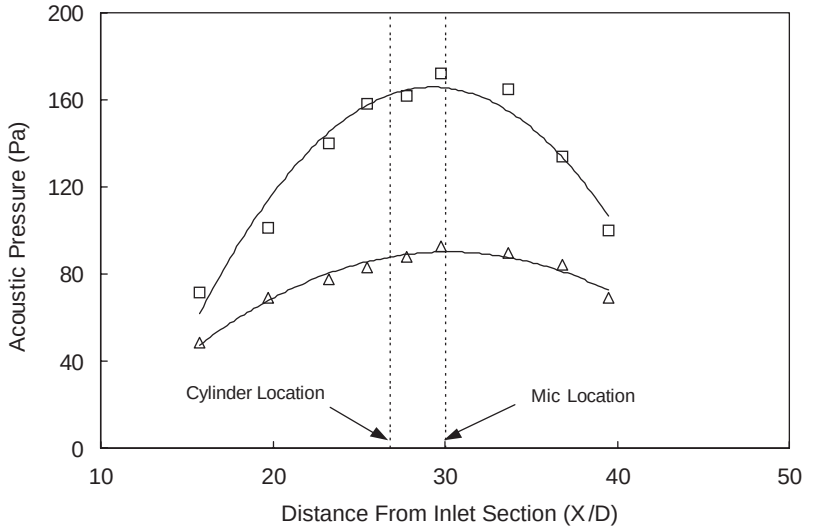

Fig. 4. Distribution of the acoustic pressure in the streamwise direction: Δ, first cross-mode, $U = 47\,\mathrm{m/s}$; □, third cross-mode, $U = 120\,\mathrm{m/s}$; $D = 12.7\,\mathrm{mm}$.

the vortex shedding frequency becomes close to that of the acoustic mode, where the lock-in phenomenon is initiated and an intense acoustic resonance is produced, as shown in Fig. 5(b). The recorded maximum sound pressure level for this case is 155.6 dB. As can be seen in Fig. 5(b), during the lock-in range, high-frequency components are also generated. These components are not the higher acoustic modes ($f(2\lambda/2), f(3\lambda/2), f(4\lambda/2), \ldots$) but rather the higher harmonics of the first acoustic mode ($2f(\lambda/2), 3f(\lambda/2), 4f(\lambda/2), \ldots$). These higher harmonics are generated by nonlinear effects due to the very high acoustic pressure at resonance. Fig. 6 is constructed from Fig. 5(b), and depicts the frequency and the amplitude of the vortex shedding component in pressure spectra as functions of the reduced velocity. The reduced velocity U_r presented in all figures is based on the frequency of the lowest cross-mode of the test section, f_a, as shown below:

$$U_r = \frac{U}{f_a D}. \tag{1}$$

The Strouhal number of vortex shedding for this case is 0.201, which agrees well with the values given in the literature for this range of Reynolds number. As shown in Fig. 6, the acoustic resonance is excited by the natural vortex shedding process, and it occurs over a single range of flow velocity. The maximum acoustic pressure does not occur at the velocity of frequency coincidence, but rather, at a higher reduced velocity.

Similar response was obtained for a 25.4 mm single cylinder in cross-flow. The lock-in region for this case is wider and the maximum acoustic pressure at resonance is much higher than those observed for all other tested cases of single cylinders. The results of this case can be compared with those reported by Blevins and Bressler (1993) for a cylinder of similar diameter positioned in a test-section with similar height. Fig. 7 shows this comparison for the lock-in region. As can be seen, excellent agreement is evident between the present work and that by Blevins and Bressler (1993), which was performed in a different wind tunnel and setup. As shown in Fig. 7, the recorded maximum sound pressure is similar in both cases, and the width of the lock-in region and the reduced velocity at the maximum sound pressure are almost identical. The Strouhal number for this case ($D = 25.4\,\mathrm{mm}$) in the present work is 0.199, and that reported by Blevins and Bressler is 0.205.

Similar characteristics were obtained from additional tests on single cylinders with different diameters. As the cylinder diameter is increased, the flow velocity required to excite the same resonance mode also increases, and therefore the dynamic head at resonance is higher for larger diameter cylinders. Fig. 8 shows these effects: as the cylinder diameter is increased, the lock-in range becomes wider and the maximum acoustic pressure increases by about an order of magnitude (from 259 to 2340 Pa) when the cylinder diameter is increased from 12.7 to 25.4 mm. The maximum sound pressure levels recorded for different cylinder diameters as well as the Strouhal number of vortex shedding are shown in Table 1.

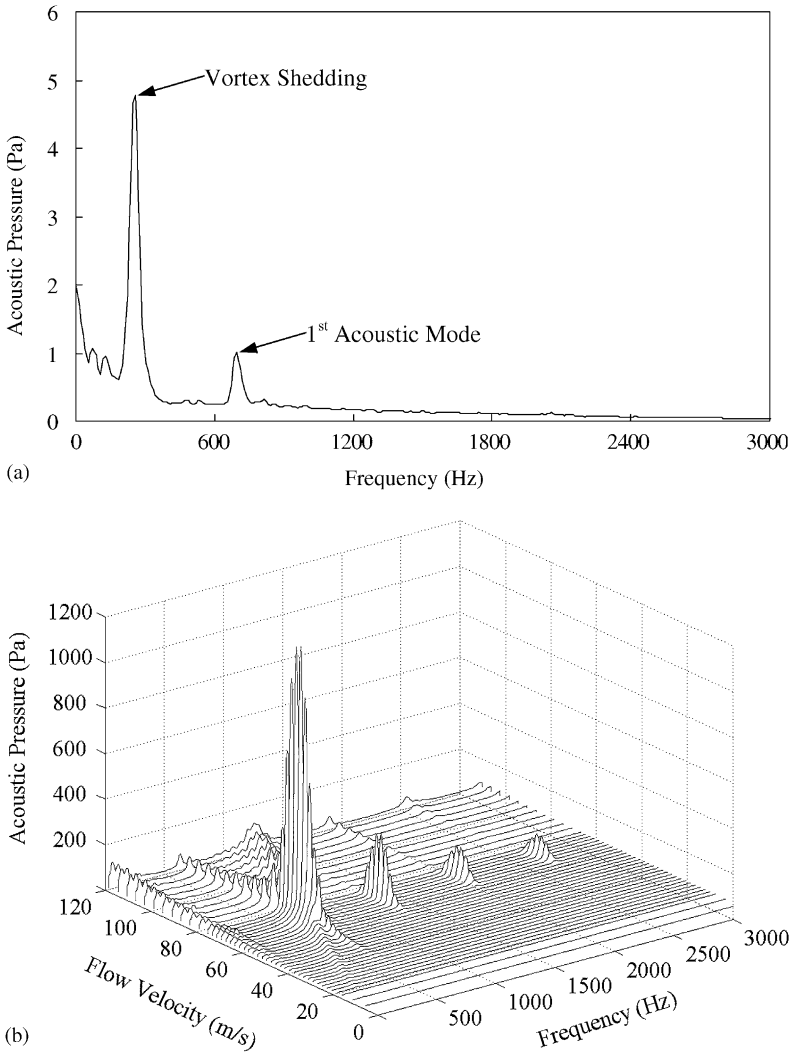

Fig. 5. (a) Pressure spectrum measured on the top wall of the test section for a single cylinder with $D = 19$ mm at a flow velocity of 25 m/s. (b) Pressure spectra for a range of flow velocities.

Based on the theory of aerodynamic sound (Lighthill, 1952), the sound generated by an eddy in a coherent flow structure is proportional to the eddy length scale, the dynamic head and Mach number. A similar expression for vortex shedding can be derived by referring to the theoretical analysis by Blake (1986). Considering a cylinder exposed to low Mach number cross-flow, and of length l which is much greater than the wavelength of the radiated sound, the far-field sound pressure radiated from the cylinder can be related to the spatial coordinates (R, θ and ϕ) and the fluctuating lift and drag coefficients (C_L and C_D) as follows:

$$p(R,\theta,\phi) = -\frac{\sin\theta\cos\phi}{4Rc}\left(\frac{\sin\eta}{\eta}\right)\rho U^3 l C_L S\cos[2\pi f_v(t-R/c)] - \frac{\sin\theta\sin\phi}{4Rc}\left(\frac{\sin 2\eta}{2\eta}\right)\rho U^3 l C_d S\cos[4\pi f_v(t-R/c)+\beta], \quad (2)$$

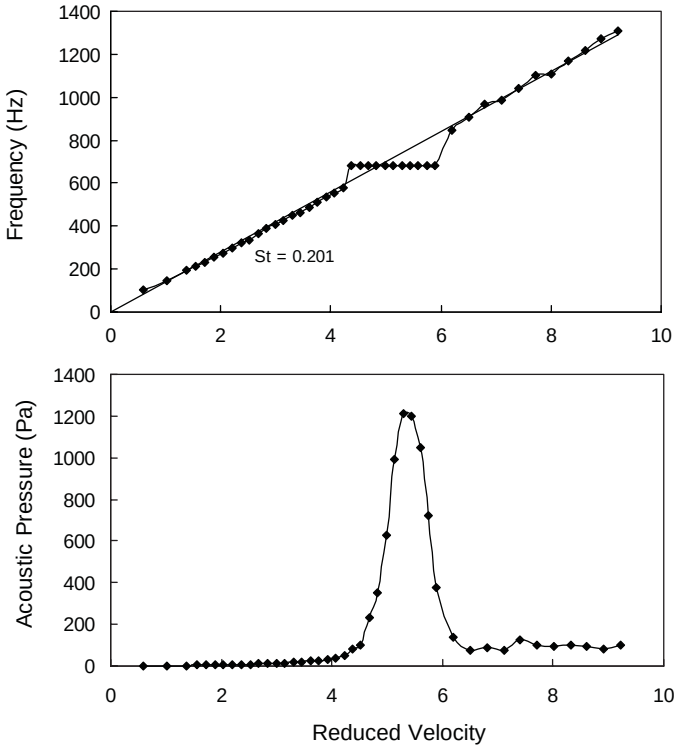

Fig. 6. Frequency and amplitude of pressure fluctuation on the test section top wall at the frequency of vortex shedding. Single cylinder tests; $D = 19\,\text{mm}$.

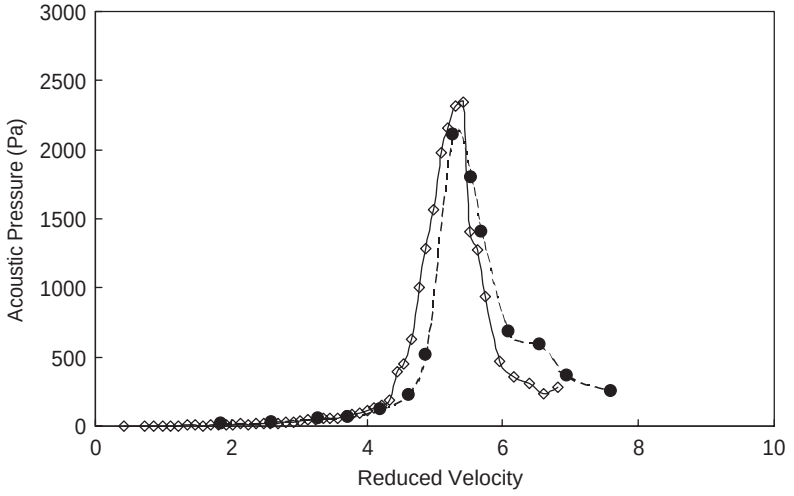

Fig. 7. Comparison of maximum sound pressure for a single cylinder; $D = 25.4\,\text{mm}$: ◇, current experiments; ●, Blevins and Bressler (1993).

where

$$\eta = \frac{kl}{2}\cos\,\theta. \tag{3}$$

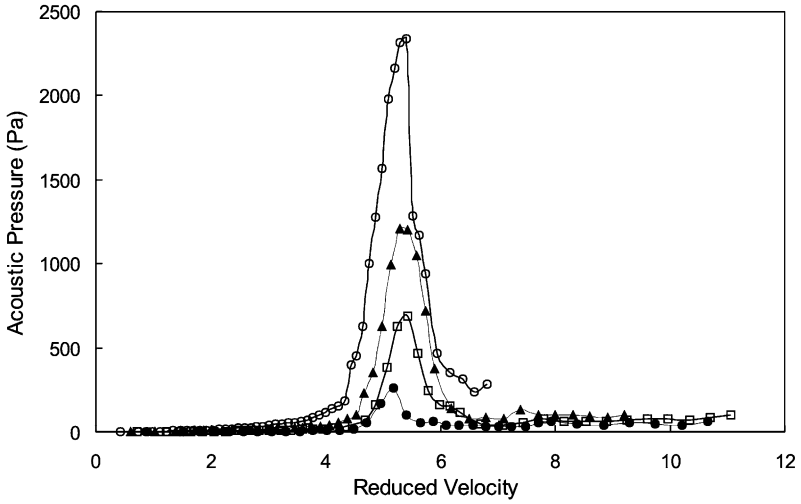

Fig. 8. Comparison of the aeroacoustic response of a single cylinder in cross-flow: ●, $D = 12.7$ mm; □, $D = 15.9$ mm; ▲, $D = 19$ mm; ○, $D = 25.4$ mm.

Table 1
Comparison of Strouhal number and maximum sound pressure level (SPL) for single cylinder tests

Cylinder diameter (mm)	12.7	15.9	19	25.4
Max SPL (dB)	142.2	150.7	155.6	161.3
Strouhal number	0.207	0.201	0.201	0.199

Furthermore, by considering the location of the microphone with respect to the cylinder, see Fig. 3, the second term in Eq. (2) vanishes, and the sound is radiated at the vortex shedding frequency f_v and at a level proportional to $\rho U^3/c$, which is the dynamic head multiplied by the Mach number. Therefore, the root mean square amplitude of the acoustic pressure (P_{rms}) is normalized by $\rho U^2 M$, i.e.,

$$P^* = \frac{P_{\text{rms}}}{\frac{1}{2}\rho U^2 M}. \tag{4}$$

By normalizing the amplitude of the acoustic pressure using Eq. (4), the scatter in the data for different cylinder diameters is greatly reduced as shown in Fig. 9. Thus, this normalization procedure seems to take into account the important parameters influencing the sound pressure of acoustic resonance due to vortex shedding from single cylinders. The small differences between the maximum values of P^* for different diameters are due to minor effects, such as the effect of the cylinder diameter on the frequency and radiation losses of the acoustic mode.

4. Acoustic resonance of tandem cylinders

4.1. Dual resonance phenomenon

For the case of two tandem cylinders in cross-flow, eleven spacing ratios from 1.2 to 4.5 were tested to study the effect of the gap between the cylinders on the excitation mechanism of acoustic resonance. Nine of these spacing ratios are within the proximity interference region, $L/D < 3.5$, and the other two are in the wake interference region, $L/D > 3.5$.

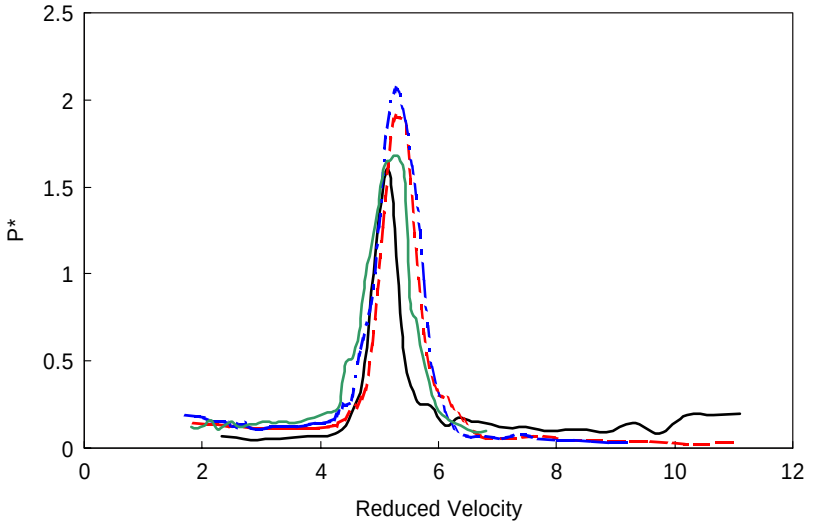

Fig. 9. Comparison of the aeroacoustic response of a single cylinder in cross-flow based on the normalized acoustic pressure: —, $D = 12.7$ mm; - - -, $D = 15.9$ mm; - · - · - ·, $D = 19$ mm; —, $D = 25.4$ mm.

These spacing ratios were carefully selected to cover different flow regimes, as discussed by Zdravkovich (1985). The investigated geometries include: three spacing ratios in the alternate reattachment regime, $L/D = 1.2$, 1.25 and 1.5; four spacing ratios in the quasi-steady reattachment regime, $L/D = 1.75$, 2, 2.25 and 2.4; two spacing ratios in the intermittent shedding regime, $L/D = 2.5$ and 3; and finally two spacing ratios in the two vortex streets regime, $L/D = 3.75$ and 4.5.

Fig. 10(a) shows a typical pressure spectrum for two tandem cylinders with a spacing ratio of 3, and Fig. 10(b) shows a water-fall plot of pressure spectra for the same spacing ratio. As in the case of a single cylinder, two frequency components are observed in Fig. 10(a), one is the vortex shedding frequency, while the other component is the first acoustic mode of the duct housing the cylinders. The aeroacoustic response of the tandem cylinders is seen to be considerably different from that of a single cylinder in cross-flow. It is observed from Fig. 10(b) that the acoustic resonance of the first mode occurs over two different ranges of flow velocity. It is also seen that the acoustic pressure during the first resonance range is higher than that generated during the second resonance range. As in the case of a single cylinder, nonlinear effects during the resonance generate the higher harmonics of the resonant mode. At a flow velocity near 90 m/s, the third resonance mode is excited, without any signs of second mode resonance.

That the second mode was not excited can be explained using the acoustic analogy developed by Howe (1975, 1984). He proposed the triple product formula

$$\Pi = -\rho \int \boldsymbol{\omega} \cdot (\boldsymbol{v} \times \boldsymbol{u}) \, \mathrm{d}\forall, \tag{5}$$

which can be used to estimate the instantaneous acoustic power, Π, generated by the convection of unsteady vorticity field, $\boldsymbol{\omega}$, within a sound field of particle velocity $\boldsymbol{u}$.

The net acoustic energy is the integration of the instantaneous acoustic power over flow volume $\forall$ for a complete acoustic cycle. Thus, the acoustic resonance would be initiated and sustained if the net acoustic energy is positive. For the second resonance mode, the acoustic particle velocity at the cylinder location is zero (particle velocity node), and hence the triple product $\boldsymbol{\omega} \cdot (\boldsymbol{v} \times \boldsymbol{u})$ is equal to zero at all times, and the net acoustic energy is also zero. For this reason the second resonance mode was not excited during the tests.

The main features of the aeroacoustic response of the tandem cylinders with $L/D = 3$ are further illustrated in Fig. 11. The Strouhal number of vortex shedding for this case is about 0.148, which is less than that of single cylinders. As the bluffness of the body increases, the Strouhal number tends to decrease; see, for example, Igarashi (1981). Referring to the lock-in ranges of the first acoustic mode, one of the resonance ranges occurs post the condition of frequency coincidence. This resonance range seems to be excited by the natural vortex shedding observed in the absence of acoustic resonance, which is similar to the case of a single cylinder. However, its normalized maximum acoustic pressure is smaller than that of a single cylinder. The other resonance range, which is the pre-coincidence resonance,

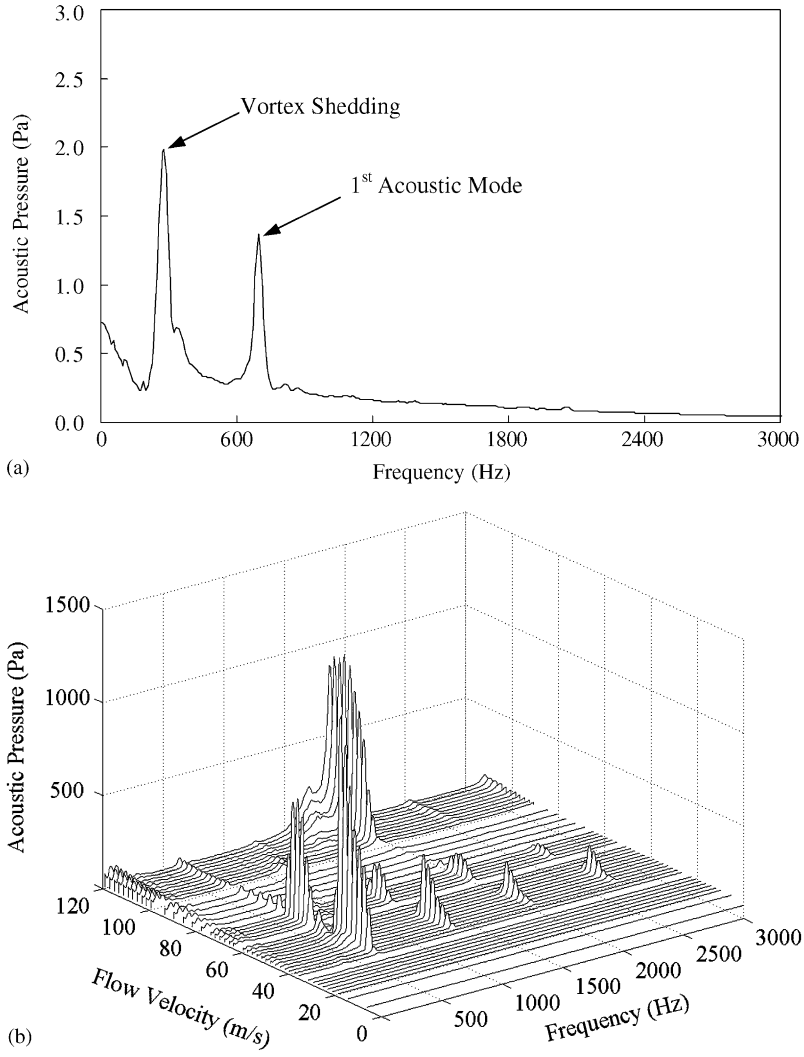

Fig. 10. (a) Pressure spectrum for two tandem cylinders; $U = 25\,\mathrm{m/s}$, $D = 12.7\,\mathrm{mm}$, $L/D = 3$. (b) Pressure spectra for a range of flow velocities.

occurs at a higher Strouhal number (i.e. at a lower reduced velocity). The normalized maximum acoustic pressure of this resonance range is stronger than that of the post-coincidence resonance range.

The multiple occurrence of resonance of a given acoustic mode, as illustrated in Fig. 11 for the first mode, will be referred to hereafter as the dual resonance phenomenon. This phenomenon can be clearly seen also in Fig. 12, which illustrates the aeroacoustic response for two tandem cylinders with a spacing ratio of 1.2. As the flow velocity is increased, the frequency of the vortex shedding component and its amplitude are increased, until the reduced velocity reaches a value of 3.58 at which the first resonance range is initiated and an acoustic resonance is produced. In this case, the pre-coincidence resonance range is not sustained for a wide range of reduced velocities as observed in the previous case, but rather it subsides at a reduced velocity of 4.51. At a higher reduced velocity, the second resonance range is initiated and a strong acoustic resonance is produced. The maximum amplitude of the normalized acoustic pressure for the first resonance range is 2.83, while that for the second resonance range is 1.24. The Strouhal number for this case is strongly dependent on the Reynolds number and it decreases in a nonlinear fashion, as shown in Fig. 12.

The dual resonance phenomenon persisted for all other tests with spacing ratios within the proximity interference region. Two examples are shown in Fig. 13 for tandem cylinders with spacing ratios of 1.75 and 2.25. The results are

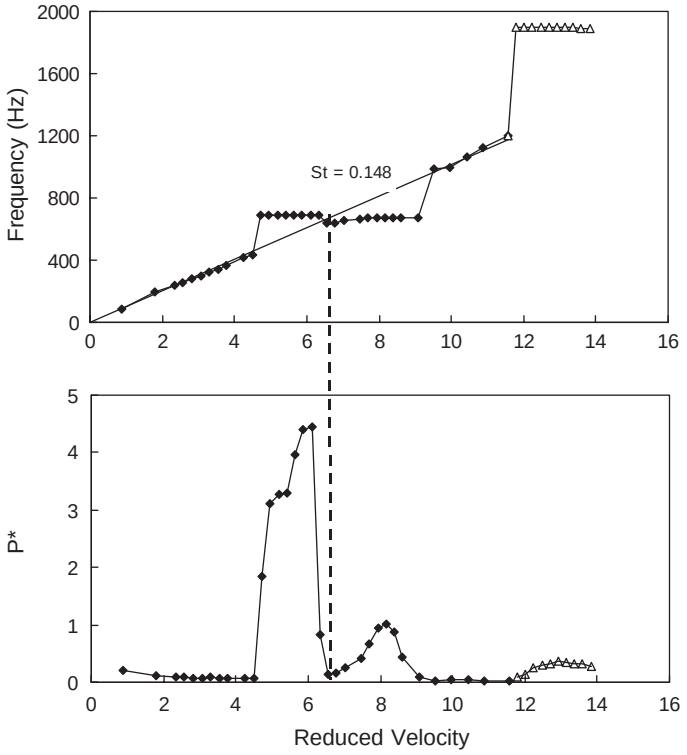

Fig. 11. Aeroacoustic response of two tandem cylinders for $L/D = 3$; $D = 12.7$ mm: ◆, first resonance mode; △, third resonance mode.

similar to those of tandem cylinders with spacing ratios of 1.5, 2, 2.4, and 2.5. In some cases, the two resonance ranges are merged together, which looks like a wide lock-in region with two pressure peaks and minimum acoustic pressure almost at the velocity of frequency coincidence, for example, for $L/D = 2.25, 2.4, 2.5$ and 3. Table 2 shows the reduced velocities at the onset of both the pre- and post-coincidence resonance ranges for all the tested cases within the proximity interference region.

4.2. Origin of the pre-coincidence resonance

At the flow velocity corresponding to frequency coincidence, the acoustic pressure of the second resonance range starts to increase, and reaches its maximum value at a higher reduced velocity, which is similar to the trend observed for a single cylinder. Thus, this range of resonance seems to be excited by vortex shedding in the wake of the rear cylinder. The first resonance range, however, is initiated at a Strouhal number which is substantially higher than that associated with the natural vortex shedding. Additionally, the resonance subsides as the reduced velocity approaches that of frequency coincidence.

A comparison between the Strouhal number of vortex shedding and that at the onset of resonance for both the pre- and the post-coincidence ranges is shown in Fig. 14. The Strouhal number in this figure is based on the distance between the cylinders, $f_a L/U$, instead of the cylinder diameter. Fig. 14 shows that the Strouhal number at the onset of resonance for the post-coincidence range is almost identical to that of vortex shedding. On the other hand, the Strouhal number at the onset of the pre-coincidence resonance is substantially higher than that of the post-coincidence range. Its value increases with the spacing ratio but remains within the range of 0.4–0.6, with the exception of the smallest spacing case. This range of Strouhal number is similar to that observed for deep cavity resonance (Ziada and Shine, 1999). In fact, the orientation of the excited acoustic mode with respect to the shear layers in the gap between the tandem cylinders is analogous to the acoustic mode of deep cavities interacting with the shear layer at the cavity mouth. Based on this analogy, it is suggested that the instability of the shear layers in the gap between the cylinders, which is analogous

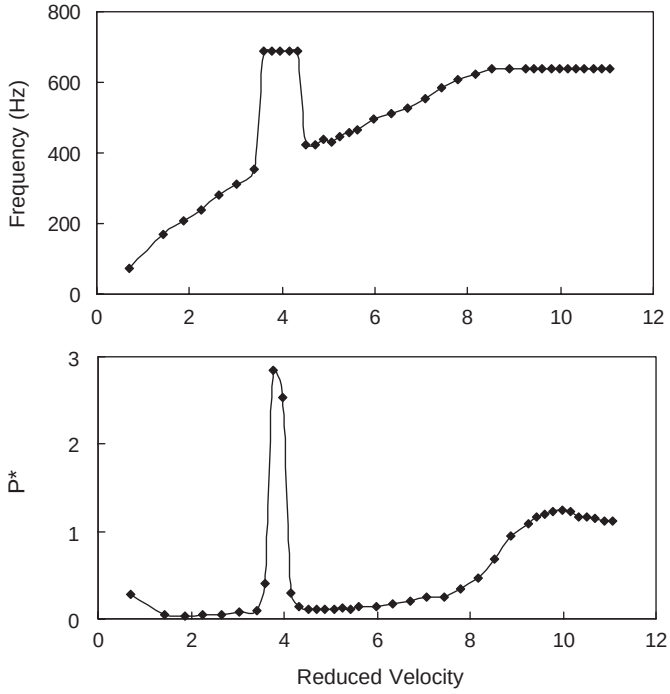

Fig. 12. Aeroacoustic response of two tandem cylinders. $L/D = 1.2$; $D = 15.9$ mm.

to the shear layer at the mouth of a deep cavity, is the dominant excitation source causing, or at least triggering, the pre-coincidence resonance range. This supposition is currently being evaluated by means of flow visualization techniques.

A direct comparison between the acoustic resonance of single and tandem cylinders is shown in Fig. 15. The x-axis in this figure is the Strouhal number of vortex shedding multiplied by the reduced velocity, which represents the ratio between vortex shedding and acoustic resonance frequencies. The onset of the pre-coincidence resonance range for the tandem cylinders is much more abrupt than the post-coincidence resonance range or the resonance of the single cylinder. It is also seen that the lock-in range for the tandem cylinders is much wider and the amplitude of the acoustic resonance is higher than those in the single cylinder case.

Fig. 16 shows the resonance intensity for different spacing ratios of the tandem cylinders. As suggested by Blevins and Bressler (1993), the normalized maximum sound pressure in this figure is combined with the ratio between the cylinder diameter to the test section height, D/H. It is seen that the normalized maximum pressure amplitudes for the post-coincidence resonance range are almost within the amplitude range of single cylinders. However, the maximum sound pressure in the pre-coincidence range is substantially higher than that of the other resonance range.

As the spacing ratio between the cylinders is increased beyond 3.5, the flow pattern changes to that corresponding to the wake interference regime. The aeroacoustic response at these large spacing ratios is found to be similar to that of a single cylinder. A typical example for $L/D = 4.5$ is shown in Fig. 17. Tests with $L/D = 3.75$ showed similar results and are not given here for brevity. It is also observed that as the spacing ratio is increased, the Strouhal number increases towards 0.2 and the amplitude of the maximum acoustic pressure decreases, which indicates a transition to the single cylinder features.

The present results of tandem cylinders within the proximity interference region clearly indicate that prediction of the critical velocity for the onset of acoustic resonance, based on the Strouhal number of natural vortex shedding, could give a ''dangerously'' overestimated critical velocity. For example, considering the case in Fig. 13(a), the observed Strouhal number of vortex shedding ($St = 0.145$) would yield a critical reduced velocity of about 6 for the onset of acoustic resonance near the frequency coincidence. As seen from the results in Fig. 13(a), the first resonance occurs at a reduced velocity of 3.5, which is about 40% lower than the predicted value from the condition of frequency coincidence.

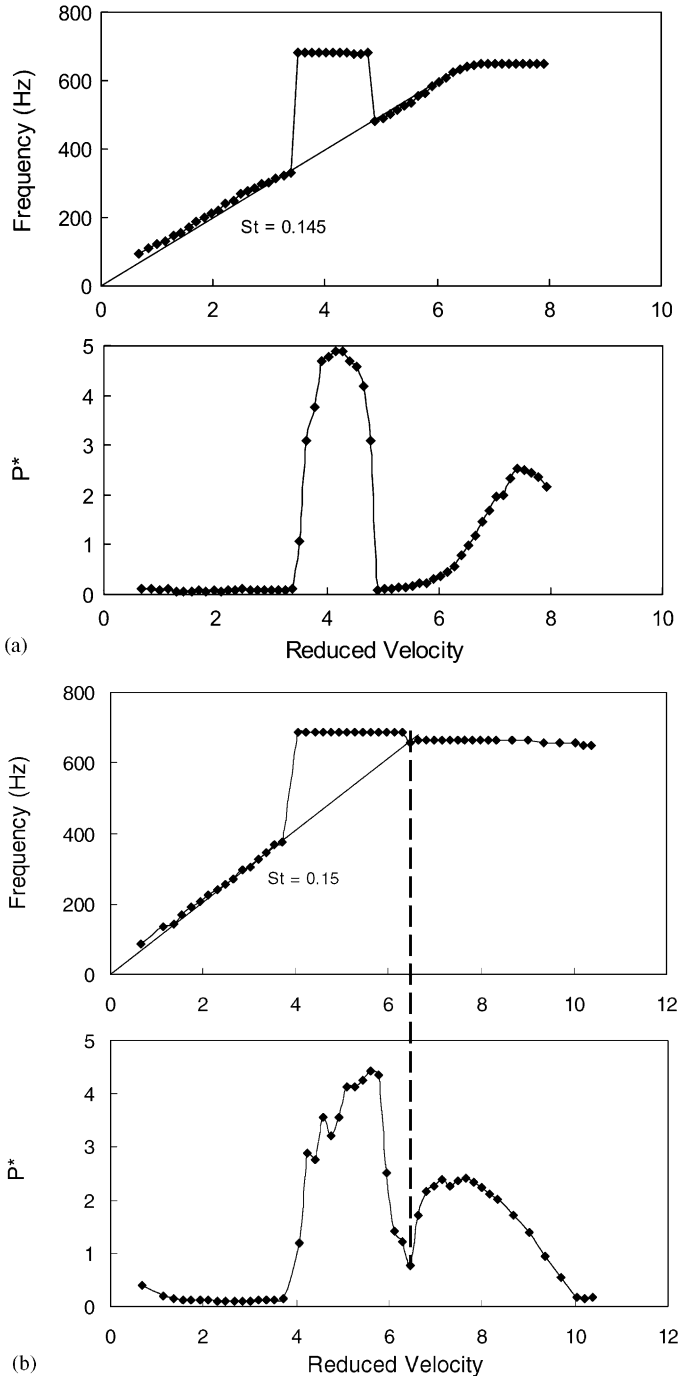

Fig. 13. (a) Aeroacoustic response of two tandem cylinders: (a) $L/D = 1.75$; $D = 21.8$ mm; (b) $L/D = 2.25$; $D = 17$ mm.

4.3. Effect of Reynolds number on Strouhal number

As mentioned earlier, the frequency of vortex shedding from two tandem cylinders does not always increase linearly with the flow velocity, especially at low Re and small spacing ratios. The effect of Reynolds number on the Strouhal number of vortex shedding from two tandem cylinders is shown in Fig. 18. The present data agree well with those in the

Table 2
Reduced velocity at the onset of the first and the second resonance ranges

L/D	1.2	1.25	1.5	1.75	2	2.25	2.4	2.5	3
U_r at the onset of pre-coincidence resonance	3.58	3.74	3.51	3.51	3.60	4.05	4.33	4.46	4.48
U_r at the onset of post-coincidence resonance	7.44	7.54	7.04	5.65	5.89	6.46	6.7	7.17	7.01

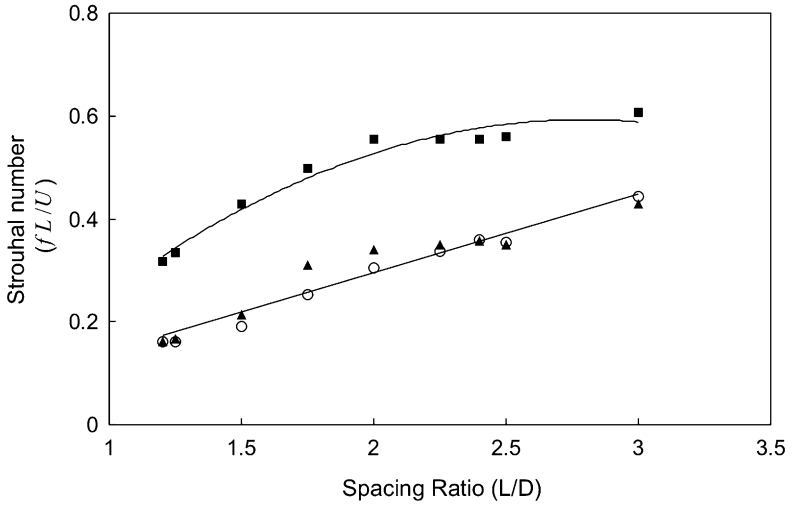

Fig. 14. Comparison of Strouhal number of vortex shedding and Strouhal number at the onset of resonance for both the pre-coincidence range and the post coincidence range. ■, Strouhal number for pre-coincidence; ▲, Strouhal number for post-coincidence; ○, Strouhal number of vortex shedding. All values of Strouhal number are based on L.

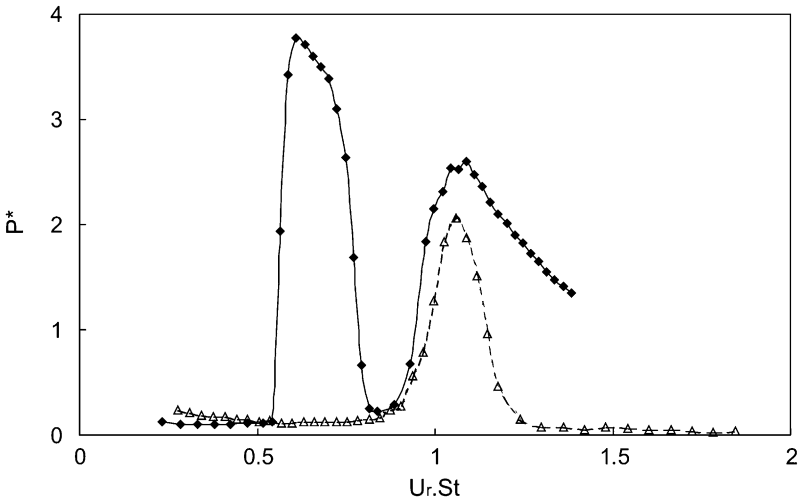

Fig. 15. Comparison of the aeroacoustic response of a single cylinder and two tandem cylinders: ◆, two tandem cylinders, $L/D = 2$; △, single cylinder; $D = 19$ mm in both cases.

literature; e.g. Hall et al. (2003) for $L/D = 1.75$ and Igarashi (1981) for $L/D = 2.06$. At high Reynolds number, above 5×10^4, the Strouhal number seems to become constant at a value of 0.15 ± 0.003, and thereby remains independent of Reynolds number and the spacing ratio between the cylinders. This finding is valid only for a spacing ratio in the range of 1.2–3.0.

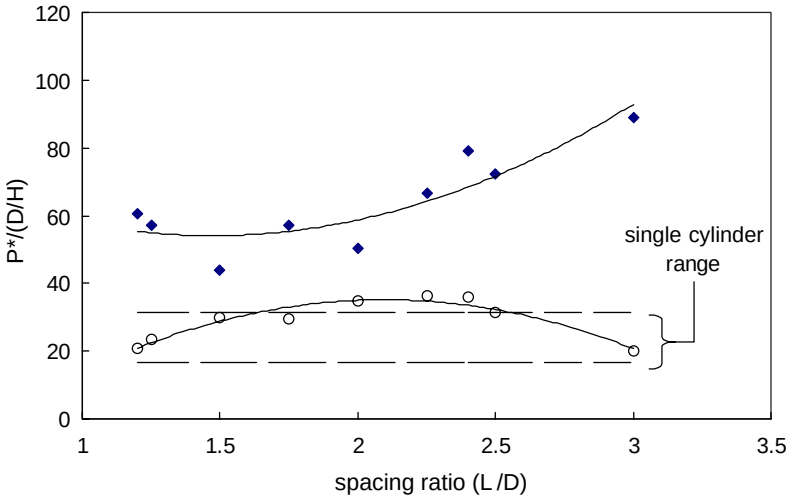

Fig. 16. Comparison between the normalized maximum acoustic pressure for the two resonance ranges: ◆, pre-coincidence; ○, post-coincidence.

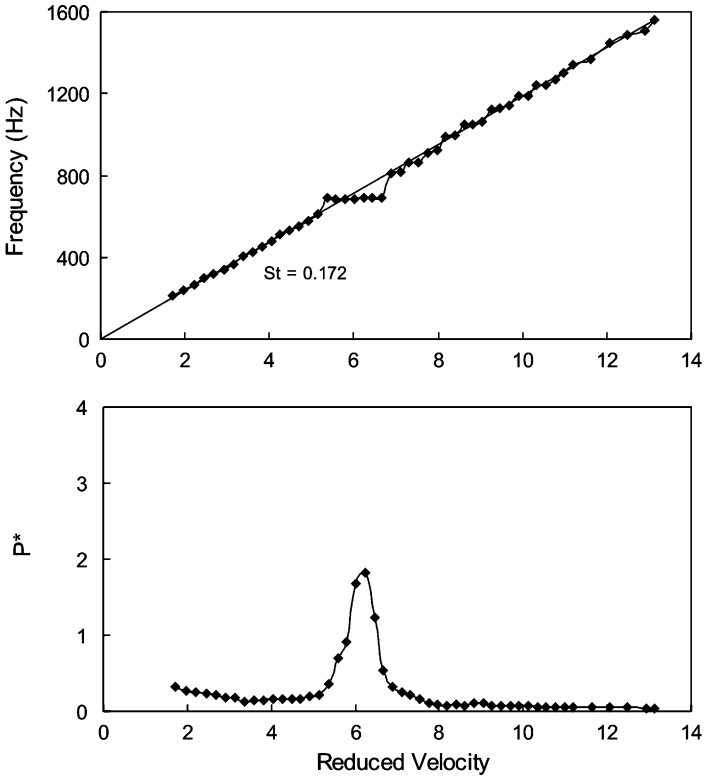

Fig. 17. Aeroacoustic response of two tandem cylinders. $L/D = 4.5$; $D = 12.7\,\text{mm}$.

5. Conclusion

The excitation of acoustic resonance by vortex shedding from two tandem cylinders in cross-flow has been investigated and the results are compared with those of a single cylinder. Four different diameters for the single cylinder

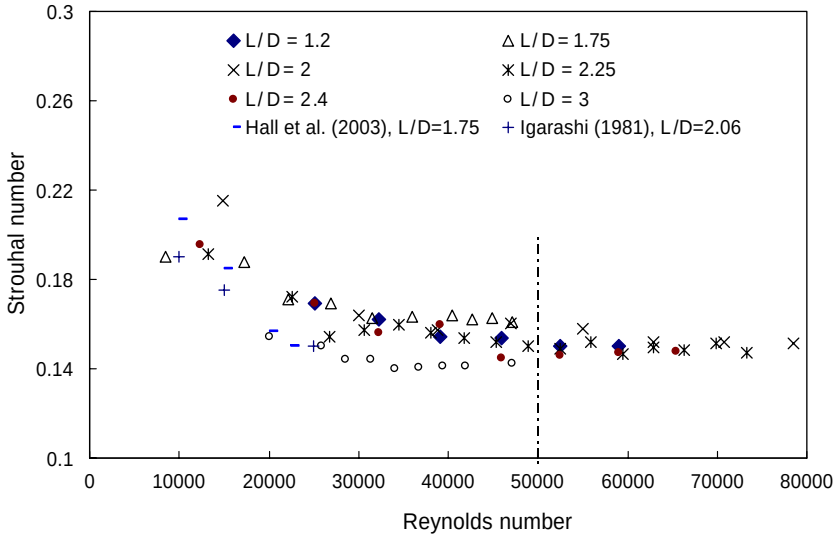

Fig. 18. Effect of Reynolds number on the Strouhal number of vortex shedding from two tandem cylinders in cross-flow with spacing ratios in the range of $1.2 < L/D < 3$.

case, and eleven spacing ratios from 1.2 to 4.5 for the tandem cylinders were tested in this study. The following conclusions are drawn:

(i) The aeroacoustic response of a single cylinder is similar to that reported in the literature. Acoustic resonance is excited by the natural vortex shedding observed before the onset of resonance. The Strouhal number of vortex shedding is 0.2 ± 0.005.
(ii) As the diameter for the single cylinder is increased, the required flow velocity to excite the acoustic resonance increases, which results in a stronger acoustic resonance and a wider lock-in range of flow velocity. The maximum sound pressure during resonance scales fairly well with the product of the dynamic head and Mach number.
(iii) The acoustic resonance of the tandem cylinders within the proximity interference region occurs over two different velocity ranges. The one occurring at higher reduced velocities is excited by the natural vortex shedding process, as in the single cylinder case. The other range is initiated at a much lower reduced velocity, and appears to be excited by the shear layers which form in the gap between the two cylinders.
(iv) For tandem cylinders with spacing ratios within the proximity interference region, the Strouhal number depends on Reynolds number. However, at high Reynolds numbers, above 5×10^4, the Strouhal number neither depends on the Reynolds number nor the spacing ratio.
(v) The aeroacoustic response of two tandem cylinders with spacing ratio in the wake interefernce region is similar to that of an isolated cylinder.

References

Blevins, R.D., 1985. The effect of sound on vortex shedding from cylinders. Journal of Fluid Mechanics 161, 217–237.
Blevins, R.D., Bressler, M.M., 1993. Experiments on acoustic resonance in heat exchanger tube bundles. Journal of Sound and Vibration 164, 503–533.
Blake, W.K., 1986. Mechanics of Flow-induced Sound and Vibration. Academic Press, New York.
Curle, N., 1955. The influence of solid boundaries upon aerodynamic sound. Proceedings of the Royal Society of London, Series A 231, 505–514.
Fitzpatrick, J.A., 2003. Flow/acoustic interaction of two cylinders in cross-flow. Journal of Fluids and Structures 17, 97–113.
Hall, J.W., Ziada, S., Weaver, D.S., 2003. Vortex shedding from single and tandem cylinders in the presence of applied sound. Journal of Fluids and Structures 18, 741–758.
Howe, M.S., 1975. Contributions to the theory of aerodynamic sound, with application to engine jet noise and theory of the flute. Journal of Fluid Mechanics 71, 625–673.

Howe, M.S., 1984. On the absorption of sound by turbulence and other hydrodynamic flows. IMA Journal of Applied Mathematics 32, 187–209.

Igarashi, T., 1981. Characteristics of the flow around two circular cylinders arranged in tandem—1st report. Bulletin of the Japan Society of Mechanical Engineers (JSME) 24 (188), 323–331.

Lighthill, M.J., 1952. On sound generated aerodynamically: I. General theory. Proceedings of the Royal Society of London, Series A 211, 564–587.

Oengören, A., Ziada, S., 1998. An in-depth study of vortex shedding, acoustic resonance and turbulent forces in normal triangle tube arrays. Journal of Fluids and Structures 12, 717–758.

Parker, R., Pryce, D.C., 1974. Wake excited resonances in an annular cascade: an experimental investigation. Journal of Sound and Vibration 37, 247–261.

Parker, R., Stoneman, S.A.T., 1989. The excitation and consequences of acoustic resonances in enclosed fluid flow around solid bodies. Proceedings of the Institution of Mechanical Engineers 203, 9–19.

Welsh, M.C., Hourigan, K., Welch, L.W., Downie, R.J., Thompson, M.C., Stokes, A.N., 1990. Acoustics and experimental methods: the influence of sound on flow and heat transfer. Experimental Thermal and Fluid Science 3, 138–152.

Zdravkovich, M.M., 1977. Review of flow interference between two circular cylinders in various arrangements. ASME Journal of Fluids Engineering 99, 618–631.

Zdravkovich, M.M., 1985. Flow induced oscillations of two interfering circular cylinders. Journal of Sound and Vibration 101 (4), 511–521.

Ziada, S., Oengören, A., Vogel, H., 2002. Acoustic resonance in the inlet scroll of a turbo-compressor. Journal of Fluids and Structures 16, 361–373.

Ziada, S., Shine, S., 1999. Strouhal numbers of flow-excited acoustic resonance in side-branches. Journal of Fluids and Structures 13, 127–142.